A necessary and sufficient condition for stability in the first case is that the initial switch line intersection occurs at an attitude error rate equal to one-half of the rate increment corresponding to the fixed control impulse. This means that steady external torque will cause instability, since that exact switch line intersection will occur only as the result of a coincidence. The second case, in which both switch lines are intersected, also leads to instability.

A demonstration of instability for the first case follows. The well-known phase-plane equation for the system is

$$e = e(0) - [I/2(L_c + L_e)][\dot{e}^2 - \dot{e}(0)^2] \quad (1)$$

Another equation governs the change in error rate due to the fixed control impulse bit:

$$\dot{e} = \dot{e}(0) + \Delta\dot{e} \quad (2)$$

Consider a fixed-impulse control-torque-on trajectory originating at the right-hand switch line, followed by a control-torque-off trajectory that ends at the same switch line. By appropriate matching of final and initial values, Eqs. (1) and (2) can be combined to yield the following difference equation for successive values of error rate at switching:

$$\dot{e}_{k+1}^2 = \dot{e}_k^2 + c\Delta\dot{e}(2\dot{e}_k + \Delta\dot{e}) \quad (3)$$

A stable limit cycle is obtained when $\dot{e}_k = -\Delta\dot{e}/2$. This condition, which specifies that the error rate at switching is one-half of the change in error rate due to a fixed control impulse, yields the stable limit cycle solution

$$\dot{e}_{k+1} = \dot{e}_k \quad (4)$$

A dimensionless perturbation form of Eq. (3) is obtained with Eq. (4) as the reference motion by the following substitution:

$$x_k = \dot{e}_k/(\Delta\dot{e}/2) + 1 \quad (5)$$

Equation (3) becomes

$$x_{k+1}^2 - 2x_{k+1} = x_k^2 + x_k(4c - 2) \quad (6)$$

Equation (6) is a nonlinear difference equation whose solution is not obvious. Adopting the Liapunov method, a positive definite function $V(x_k)$ is found whose first difference ΔV is positive over the region of interest but zero at the origin, proving instability. The positive definite function and its first difference are

$$V(x_k) = x_k^2/2 \quad (7)$$

$$\Delta V(x_{k+1}, x_k) = x_{k+1} + x_k(2c - 1) \quad (8)$$

$$\Delta V(x_k) = 1 - [(1 - x_k)^2 + 4cx_k]^{1/2} + x_k(2c - 1) \quad (9)$$

The minus sign before the bracket corresponds to the physical fact that the switch line is unsymmetrical. Figure 2 shows that ΔV is positive everywhere in the region of interest ($x_k < 1.0$, $c > 1.0$), except at $x_k = 0$, proving instability.[3]

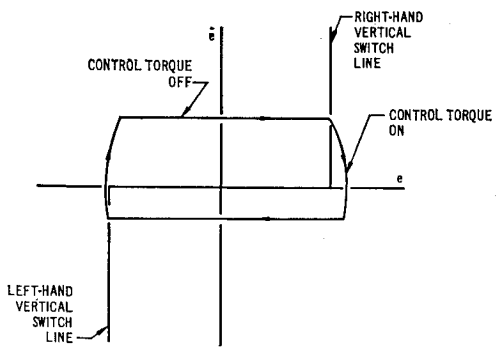

Fig. 1 A limit cycle for unsymmetrical vertical switch line fixed-impulse-bit attitude control system.

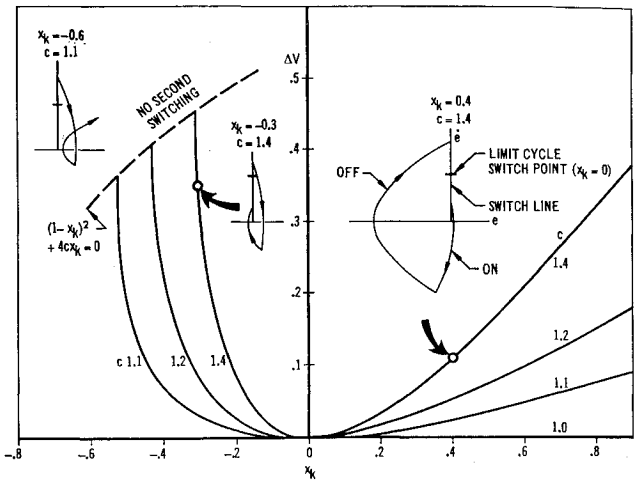

Fig. 2 Variation of the difference function ΔV with x_k and c.

The left-hand sketch of Fig. 2 is representative of trajectories having x_k and c values to the left of the dotted line labeled "no second switching." The trajectories following the initial switching at x_k do not intersect the switch line again but "escape" to the right. The other sketches illustrate two terms of the divergent series implied by $\Delta V > 0$.

References

[1] Gaylord, R. S. and W. N. Keller, "Attitude control system using logically controlled pulses," *Guidance and Control*, edited by R. E. Roberson and J. S. Farrior (Academic Press, New York, 1962), Chap. H, pp. 629–648.

[2] Twombly, J. W., "The Mercury capsule attitude control system," *Proceedings of the National Meeting on Manned Space Flight* (Institute of the Aerospace Sciences, New York, 1962), pp. 228–231.

[3] Hahn, W., "On the application of the second method of Lyapunov to difference equations," translation by G. A. Bekey, STL Rept. TR-61-5110-16 (April 1961).

Correlation of Rocket Nozzle Gas Injection Data

JAMES E. BROADWELL*
Space Technology Laboratories, Inc., Redondo Beach, Calif.

WALKER, Stone, and Shandor[1] report the results of an extensive experimental investigation of the effects of injectant molecular weight and injectant nozzle diameter on the side force induced in a rocket nozzle by secondary injection. Reference 2 contains an analysis of this problem that predicts the effect of injectant molecular weight and concludes that the interaction force (the side force minus the force arising directly from the injection momentum) is independent of injectant pressure over a wide range of pressure and, hence, independent of injectant nozzle diameter. It is the purpose of this note to compare these results.

In the experiment described in Ref. 1, the side force was measured by force transducers in a conical rocket nozzle in which the propellant was decomposed H_2O_2, and several gases (CO_2, N_2, Ar, He, and H_2) at ambient temperature were injec-

Received April 29, 1963.

* Associate Manager, Aerosciences Laboratory Research Staff, Space Technology Laboratories, Inc. Member AIAA.

Table 1 Properties of rocket motor, nozzle, and injectants used in experiments

Motor	
Propellant	90% H_2O_2
Exhaust gas composition	0.708 mole fraction H_2O 0.292 mole fraction O_2
Chamber pressure	≈400 psi
Propellant flow rate	≈0.84 lbm/sec
Exhaust gas total temperature T_{T_∞}	1845°R
Specific heat ratio γ	1.266
Ambient pressure	atmospheric
Injectant	
Injectant pressure $(P_T)_j$	40 to 1000 psi
Injectant total temperature T_{Ti}	≈70°F
Nozzle (conical, sharp-edged throat)	
Divergent half angle	15°
Throat diameter	0.501 in.
Exit diameter	1.074 in.
Nozzle diameter at injectant port	0.812 in.
Mach number at injection plane M_∞	2.34

tants. Injection was through circular orifices, of several different diameters, normal to the primary nozzle axis. Table 1 contains most of the details of the arrangement.

In the analysis[2] the interaction force, F_i, is given by

$$F_i = 1.2\,\sigma(\gamma)\,M_\infty V_\infty \left[1 + \frac{[2 + (\gamma - 1)M_\infty^2]}{2(\gamma - 1)M_\infty^2}\frac{n_\infty}{n_i}\frac{T_{Ti}}{T_{T\infty}}\right] m_i \quad (1)$$

in which 1.2 is a constant determined empirically from experiments described in Ref. 2, $\sigma(\gamma)$ is a parameter determined in blast wave theory, γ is the primary gas specific heat ratio, M_∞ and V_∞ are the Mach number and velocity of the primary flow at the injection station, n is the molecular weight, T_T is the total temperature, and m_i is the injection rate. The subscript i refers to the injectant and ∞ to the freestream. This expression gives the force on a flat plate, i.e., it is not corrected for nozzle wall curvature, and hence it applies only at low flow rates.

The total side force is obtained by adding to F_i the injection reaction force F_j given by

$$F_j = m_i V_j + (p_i - p_\infty)A_j \quad (2)$$

where V_j is the injection velocity, p_j is the pressure at the injection nozzle exit, p_∞ is the undisturbed primary nozzle pressure at the injection station, and A_j is the injector area. When the injector pressure ratio $(p_T)_j/p_\infty$ exceeds the critical ratio, the reaction force, denoted by F_j^*, is given by

$$F_j^* = m_i V_j\,[(\gamma_i + 1)/\gamma_i] - p_\infty A_j \quad (3)$$

where γ_i is the injectant specific heat ratio.

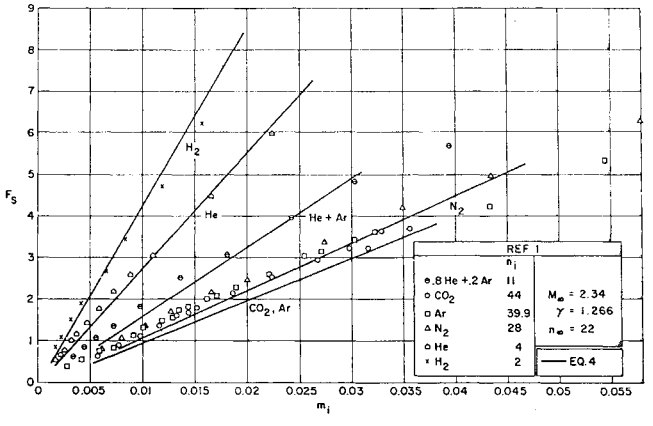

Fig. 1 Side force in pounds vs injectant mass flow in pounds mass per second; injector diameter is 0.0625 in.; effect of injectant molecular weight.

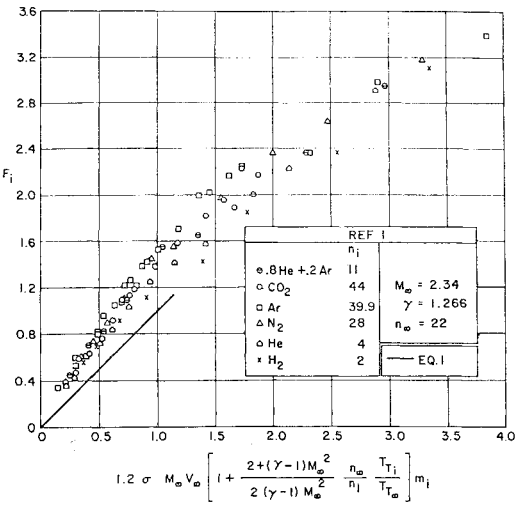

Fig. 2 Interaction force in pounds vs effective injectant mass flow in pounds.

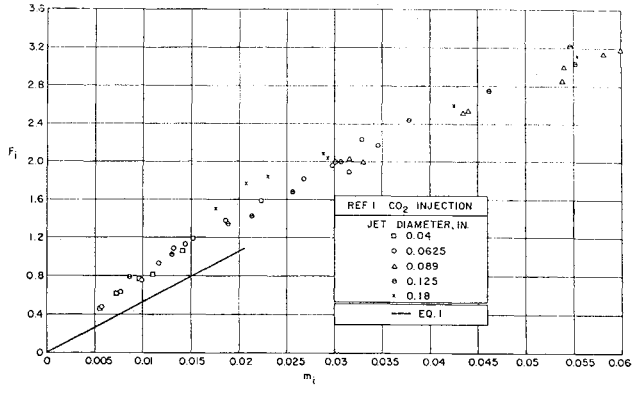

Fig. 3 Interaction force in pounds vs injectant mass flow in pounds mass per second; effect of injectant port diameter (or pressure).

The actual pressure in the neighborhood of the injector is, of course, not equal to p_∞ because of the disturbance to the primary stream. Therefore, except at high injection pressure ratios, F_j is not the actual reaction to the injection momentum, and the division of the side force into F_i and F_j is somewhat formal. The results obtained in Ref. 2, as well as those discussed below, show the usefulness of the division.

In Fig. 1 the measured side force is compared with the analytical prediction

$$F_s = F_i + F_j^* \quad (4)$$

in which F_j^* appears, even when the injector actually is not choked, because $(p_T)_j/p_\infty$ exceeds the critical ratio in all these experimental runs. From the primary gas properties, V_∞ was estimated to be 4100 fps and $\sigma(\gamma)$ to be 0.13. The injectant total temperature T_{Ti} was 70° F, M_∞ was 2.34, and the injectant port diameter was 0.0625 in.

The general dependence of the side force on the flow rate and the molecular weight is seen to be given quite accurately by the analysis, but the predicted magnitude of this force is somewhat low at low flow rates. The decrease in side specific impulse, F_s/m_i, with increasing m_i is shown in Refs. 2 and 3 to come from the spread of the high pressure region out of the plane of the injector. As stated, this geometrical effect has not been included in the analysis.

In Fig. 2 the accuracy with which the analysis determines the effect of molecular weight on the induced force alone is shown more clearly. Here, the measured induced force is plotted against an effective mass flow, the right-hand side of

Eq. (1), instead of m_i. It is seen that the correlation provided by Eq. (1) is excellent at low and high flow rates but only fair at the intermediate values. The correlation on the whole is, however, greatly superior to that proposed in Ref. 1. Note that it is important to plot the data as shown and not as an effective force, F_i divided by the coefficient of m_i in Eq. (1), vs m_i, for the effect of wall curvature just mentioned depends strongly on the magnitude of the force. As pointed out earlier, the predicted magnitude of the interaction force is lower than the measured.

Consider next the effect of injection total pressure, or injectant nozzle diameter, on side force at a fixed injection rate. The injection momentum obviously depends on these variables, in fact, when the nozzle is choked the momentum depends directly on A_j as Eq. (3) shows. It is argued in Ref. 2 that it is only through this dependence that F_s is affected by A_j, i.e., that F_i is independent of this variable. In the experiments, CO_2 was introduced through various diameter ports and F_s measured. In Fig. 3 the measured F_s minus F_j or F_j* is plotted as a function of mass flow. It is seen that there is no systematic dependence of F_i on d_i; on the contrary, except for the region around $m_i = 0.02$ lbm/sec, F_i is independent of d_i.

In summary, it is concluded that the analysis in Ref. 2 provides the basis for a good correlation of the experimental data of Ref. 1; in particular, the dependence of the side force on injectant molecular weight and injectant pressure is predicted correctly by the analysis. On the other hand, the magnitude of the predicted side force is low. A possible explanation for the discrepancy is that the experimental Mach number is too low for the blast wave theory, on which the analysis rests, to yield accurate quantitative results.

References

[1] Walker, R. E., Stone, A. R., and Shandor, M., "Secondary gas injection in a conical rocket nozzle," AIAA J. 1, 334–338 (1963); see also Ref. 24 of this paper.

[2] Broadwell, J. E., "An analysis of the fluid mechanics of secondary injection for thrust vector control (revised)," Space Technology Labs. Rept. 6120-7744-MU-000 (March 15, 1962); also AIAA J. 1, 1067–1075 (1963).

[3] Newton, J. R., Jr. and Spaid, F. W., "Interaction of secondary injectants and rocket exhaust for thrust vector control," ARS 32, 1203–1211 (1962).

Results of Ranger 1 Flight Friction Experiment

J. B. Rittenhouse,* L. D. Jaffe,† R. G. Nagler,‡ and H. E. Martens§
Jet Propulsion Laboratory,
California Institute of Technology, Pasadena, Calif.

An experiment to measure coefficients of friction in space was flown on the spacecraft Ranger 1 and 2, with the intent of making measurements under a vacuum better than can be obtained on earth under conditions of practical laboratory use. The apparatus, shown in Fig. 1, consisted essentially of 20 specimen disks mounted on a drive shaft, with four hemispherical specimen riders ($\frac{1}{8}$-in. diam) rubbing against each disk. The shaft was driven at 3 rpm by a sealed gear-motor. Each rider was held against a disk with a load of 0.3 lb provided by a calibrated coil spring; the frictional force was measured by the deflection of a leaf spring, supporting the rider, to which strain gages were attached. The strain gage output, telemetered to earth, indicated the coefficient of friction between rider and disk.

Two to four replicates of each rider-disk combination were used. The choice of materials was constrained to minimize magnetic materials in order to avoid interference with a magnetometer experiment aboard the spacecraft. A 5-μ-in. finish was specified for all metallic specimens. After final machining, disks and riders were cleaned with methyl ethyl ketone, dried, and thereafter touched only with plastic gloves.

Comparative tests in a laboratory vacuum of about 5×10^{-6} mm Hg were made on a duplicate of the flight apparatus. The disks and riders used for flight were run for 30 min in air during the final preflight spacecraft systems test. The experiment then was turned off and was turned on again by the spacecraft timer 6 hr after launch. Rangers 1 and 2 were intended to have elliptical orbits of very high apogee. Malfunction of the second stage of the launch vehicle resulted in these spacecraft being injected into low orbits. Thus, the vacuum desired for the experiment was not attained. The initial apogee for Ranger 1 was 504 km, the perigee 170 km; the corresponding pressures were about 7.8×10^{-9} mm Hg at apogee and 2.1×10^{-6} mm Hg at perigee.[1] The orbit of Ranger 2 was lower. Telemetry indicated that on both flights the experiment started in space as scheduled. From Ranger 1, telemetered friction data were received on a number of passes beginning about 13 hr after experiment start and continuing to a shutoff (believed due to normal rundown of the experiment batteries) at about 22 hr after experiment start. On Ranger 2 only a few pieces of telemetered friction data were received, and the spacecraft re-entered about 14 hr after experiment start.

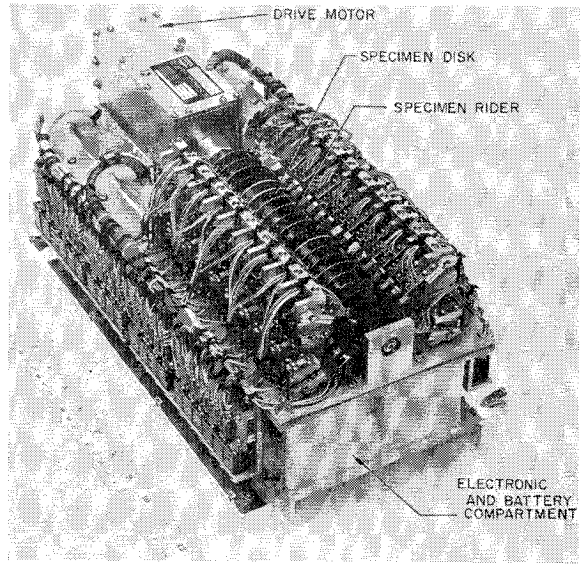

Fig. 1 Friction experiment assembly with temperature control surfaces removed.

Some noise was observed on the telemetered analog record. The "most probable" value of friction coefficient was read from the record and plotted vs time for each rider-disk combination. Figure 2 is typical data plot; dotted lines join points for each replicate. Comparisons of results in space, laboratory vacuum, and air are complicated by differences in running time. Because of the nonstandard orbit of Ranger 1, the flight data were obtained after considerably longer

Received May 20, 1963. This paper presents the results of one phase of research carried out at the Jet Propulsion Laboratory, California Institute of Technology, under Contract NAS7-100, sponsored by NASA.

* Formerly Research Specialist, Materials Research Section; now Research Scientist, Lockheed Missiles and Space Company, Palo Alto, Calif.

† Chief, Materials Research Section. Member AIAA.

‡ Research Engineer, Materials Research Section. Associate Member AIAA.

§ Assistant Chief, Materials Research Section.